Electrochemical and Catalytic Studies of Cysteine Oxidation Induced by an Organic p-n bilayer both under Illumination and in the Dark

Ryuhei Watanabe and Toshiyuki Abe[*]

Department of Frontier Materials Chemistry, Graduate School of Science and Technology, Hirosaki University, 3 Bunkyo-cho, Hirosaki 036-8561, Japan
[*]E-mail: tabe@hirosaki-u.ac.jp

As found recently by our group, dual-functional catalysis represents a specific chemical process that can induce a redox reaction not only under illumination but also in the dark. In a previous study, an organic p-n bilayer, comprising 3,4,9,10-perylenetetracarboxylic-bis-benzimidazole (PTCBI) and cobalt(II) phthalocyanine (CoPc), was utilized as a catalyst in the presence of 2-mercaptoethanol. Amino acids are attractive targets for studying dual catalysis because they bear various electron-donating groups such as –COOH, –NH$_2$, –OH, and –SH. In this work, cysteine (Cys) was subjected to dual catalysis reaction assisted by the PTCBI/CoPc bilayer. Similar to the aforementioned study, the organo-bilayer showed dual-catalytic activity for the oxidation of Cys along with the reduction of H$^+$ to H$_2$, where the Cys oxidation can be considered to occur at the top end of the valance band (Co^{III}Pc) and at the bottom end of the conduction band (Co^{II}Pc) with and without irradiation, respectively. Based on the results obtained by employing serine (Ser) as a reference compound, it appeared that the dissociated thiol group of Cys is responsible for the dual catalysis by the organo-bilayer.

1. INTRODUCTION

Photocatalysis reaction corresponds to photo-induced redox reaction, where photocatalysts are applied to a down-hill reaction ($\Delta G° < 0$, e.g., pollutants degradation) [1-5] or to an up-hill reaction ($\Delta G° > 0$, e.g., water splitting) [6-10]. Among the photocatalysts studied for the degradation of various pollutants, titanium dioxide (TiO$_2$) is the most widely utilized one [11-13]. However, TiO$_2$ is photocatalytically active only under UV light irradiation, what makes the targets for photocatalytic degradation limited to a small quantity (or a low concentration) of pollutants. Therefore, development

of novel and efficient photocatalysts, capable of degrading a large quantity of substances using wide-spectral range, will be a promising option for expanding the practical applications of photocatalysis technology.

Previously, we have investigated photocatalysis of organic p-n bilayers by applying them to various types of reactions [14-20]. Several novel photocatalytic reactions have thus far been exemplified (e.g., the visible-light-induced decomposition of hydrazine (N_2H_4) into N_2 and H_2 [17, 18], a bias-free water-splitting system of a TiO_2 photoanode featuring an organo-photocathode [19], a catalyst system that can perform the same redox reaction in the dark as well as under illumination [20], etc.). The latter work is briefly interpreted as follows [20]. When irradiating an organic p-n bilayer comprising n-type 3,4,9,10-perylenetetracarboxylic-bis-benzimidazole (PTCBI) and p-type cobalt(II) phthalocyanine (CoPc), an oxidizing power can be produced at the CoPc surface through a series of photophysical events: formation of excitons originating from light absorption by PTCBI (*vide infra*), excitation energy transfer through the PTCBI layer, generation of a carrier at the p-n interface, and transport of the hole carriers to the CoPc surface, followed by the oxidation of 2-mercaptoethanol at the oxidized CoPc (the top end of the valence band ($Co^{III}Pc$)). Furthermore, in the dark, the thiol oxidation can be induced at the bottom end of the conduction band ($Co^{II}Pc$). Moreover, the electron carriers can attain the bottom end of the conduction band of PTCBI irrespective of illumination, thus leading to the production of a reducing power for the formation of H_2 from H^+ (see Scheme 1).
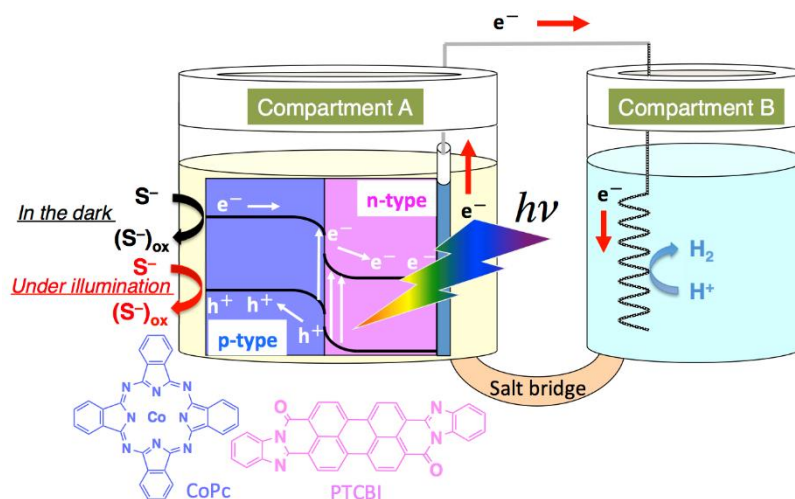
Scheme 1. The dual-functional catalysis system.

In contrast to a conventional photocatalyst, which is active only under illumination, we have demonstrated that the organo-bilayer is capable of "dual-functional catalysis", where catalytic process can initiate the redox reaction both under illumination and in the dark. This knowledge is considered to bring a novel approach to pollutants degradation by means of catalysis.

In this work, the dual catalysis by the PTCBI/CoPc bilayer was examined in the presence of amino acids. Amino acids are attractive compounds because they have various types of electron-donating groups, such as –COOH, –NH$_2$, –OH, and –SH. Cys-bearing thiol group was subjected to the dual catalysis, and Serine (Ser) was used as a reference compound. The achieved results were represented in terms of electrochemical and catalytic aspects.

2. EXPERIMENTAL

PTCBI was synthesized and purified according to the previous procedure [21]. CoPc (Tokyo Chemical Industry) was purchased and used as received. Commercially available zinc phthalocyanine (ZnPc, TCI) was used after purification by means of sublimation, as described elsewhere [17, 19]. The other reagents, including amino acids, were of the extra-pure grade and used as received. The indium-tin oxide (ITO)-coated glass plate (sheet resistance: 8 $\Omega\cdot cm^{-2}$; transmittance: >85%; ITO thickness: 174 nm) was obtained from AGC Inc.

The PTCBI/CoPc bilayer was prepared by vapor deposition (degree of pressure: ~1.0×10^{-3} Pa; deposition speed: ~0.03 nm$\cdot$s^{-1}), where PTCBI was layered on ITO, followed by coating CoPc onto the PTCBI layer (denoted as ITO/PTCBI/CoPc). Furthermore, the device with organo-trilayered structure, where ZnPc is further coated on the CoPc layer (denoted as ITO/PTCBI/CoPc/ZnPc), was prepared according to the same procedure as the organo-bilayer. During vapor deposition, the temperature of the ITO plate was not controlled. Absorption spectral measurements were conducted using a PerkinElmer Lambda 35 spectrophotometer. The thus-obtained resulting absorption spectra of PTCBI [22], CoPc [23] and ZnPc [24] were identical to those reported earlier. The thicknesses of the organo-bilayer and the trilayer were determined from the absorption spectra as described previously [20, 25-27].

For photoelectrochemical studies such as voltammogram measurements and photocurrent measurements under potentiostatic condition for acquiring an action spectrum, a single-compartment cell was employed with a modified ITO working electrode (geometrical area: 1 cm × 1 cm), a spiral Pt counter electrode, and an Ag/AgCl (in saturated KCl electrolyte) reference electrode. The measurements were conducted in an electrolyte solution containing an amino acid in an Ar atmosphere. The experiments were operated using a potentiostat (Hokuto Denko, HA-301) with a function generator (Hokuto Denko, HB-104), a coulomb meter (Hokuto Denko, HF-201), and an X-Y recorder (GRAPHTEC, WX-4000) under illumination. A halogen lamp (light intensity: ~100 mW$\cdot$cm^{-2}) was used as a light source under standard conditions. For monochromatic light irradiation, the lamp was used in combination with a monochromator (Soma Optics, Ltd., S-10). Light intensity was measured using a power meter (type 3A from Ophir Japan, Ltd.).

The incident photon-to-current conversion efficiency (*IPCE*) was calculated using the following equation:

$$IPCE \quad (\%) = ([\,I\,/\,e\,]\,/\,[\,W\,/\,\varepsilon\,]) \times 100,$$

where I (A$\cdot$cm^{-2}) is the photocurrent density, e (C) is the elementary electric charge, W (W$\cdot$cm^{-2}) is the light intensity, and ε is the photon energy of monochromatic light.

Photocatalytic experiments were performed in an Ar atmosphere using a twin-compartment cell where ITO/PTCBI/CoPc (oxidation site) and a Pt wire (reduction site) were placed in Compartments A and B, respectively (see Scheme 1). ITO/PTCBI/CoPc was immersed in an electrolyte solution containing a known concentration of amino acid and the Pt wire in a phosphoric acid solution (pH = 0). For preparation of a salt bridge, agar (1.3 g) and KNO$_3$ (4.74 g) were dissolved in hot water (1.0×10^{-2}

dm^3), and then, the mixture was allowed to flow into the bridging part of the cell and solidify at room temperature.

Potentiostatic photoelectrolysis of ITO/PTCBI/CoPc was carried out using the same electrochemical equipment and the cell as for the photocatalytic experiments, where the Ag/AgCl reference electrode was set in Compartment B (*vide infra*). The gaseous product was analyzed using a gas chromatograph (GL Sciences, GC-3200) equipped with a thermal conductivity detector and a 5-Å molecular sieve column (carrier gas, Ar).

3. RESULTS AND DISCUSSION
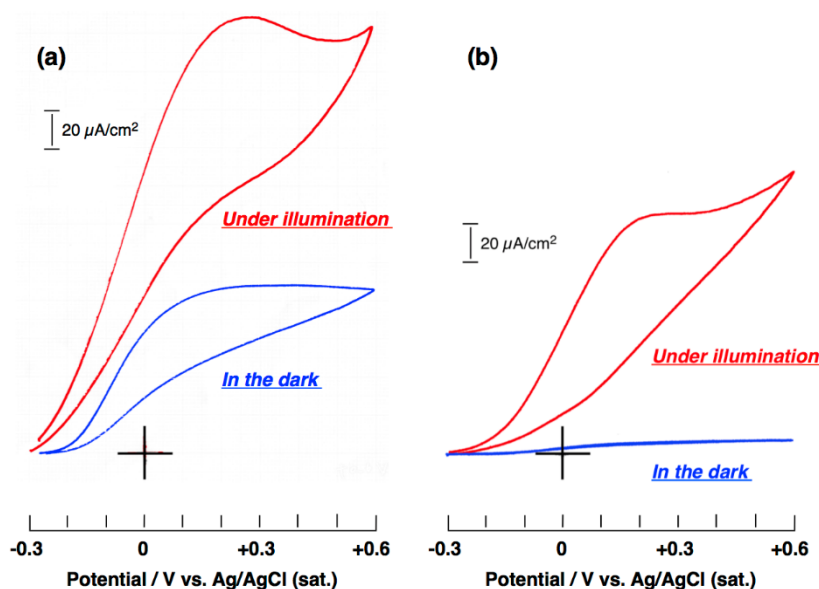
Figure 1. Cyclic voltammograms measured at ITO/PTCBI/CoPc (a) and ITO/PTCBI/CoPc/ZnPc (b). Film thickness: ~210 nm for PTCBI, ~65 nm for CoPc, and ~30 nm for ZnPc; electrolyte solution, 5 mM Cys solution (pH 10); light intensity, 100 mW·cm^{-2}; irradiation direction: from the back side of the ITO-coated face; scan rate, 20 mV·s^{-1}.

First, ITO/PTCBI/CoPc was used as the working electrode for conducting its primary evaluation in the presence of Cys, wherein voltammograms were obtained under illumination and in the dark. As shown in Fig. 1(a), a photoanodic current was present to occur at the organo-electrode. Furthermore, Fig. 1(a) represents that ITO/PTCBI/CoPc can induce the generation of an anodic current particularly in the dark. However, when employing ITO/PTCBI/CoPc/ZnPc as a control electrode, only the photoanodic response was observed (Fig. 1(b)). These results suggest that the CoPc surface in the PTCBI/CoPc bilayer is responsible for the oxidation of Cys, irrespective of irradiation. The obtained results were also in accordance with our recent report, where 2-mercaptoethanol (i.e. thiol) was used as the reductant (*vide supra*) [20]. The role of ZnPc layer will be discussed later.
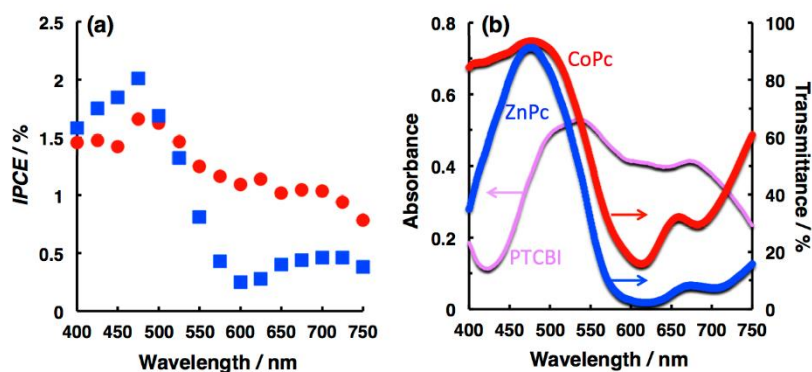
Figure 2. (a) Action spectra for photocurrents generated at ITO/PTCBI/CoPc/ZnPc (the direction of incidence: •, from the back side of the ITO-coated face; ■, from ZnPc surface). Film thickness, ~250 nm for PTCBI, ~60 nm for CoPc, and ~30 nm for ZnPc; electrolyte solution, 5 mM Cys solution (pH 10); applied potential, +0.4 V (vs. Ag/AgCl (sat.)). (b) Absorption spectrum of single-layered PTCBI, and transmittance spectra of CoPc and ZnPc.

Fig. 2(a) shows the results of action spectral measurements with respect to incidence directions, where ITO/PTCBI/CoPc/ZnPc was used as the photoanode. The action spectrum obtained after irradiation with monochromatic light from the back side of the ITO-coated face was consistent with the absorption spectrum of PTCBI (Fig. 2(b)). Furthermore, the incidence from the ZnPc surface resulted in the agreement of the action spectrum (a) with the transmittance spectra of phthalocyanines (b), indicating that the absorption of phthalocyanines can scarcely induce the generation of photocurrents. According to previous observations [28], the achieved results demonstrated that the quantitative quenching of excited PTCBI occurs in the presence of a phthalocyanine layer, suggesting that carrier generation at the p-n interface can be caused by the sole absorption of PTCBI. In order to clarify the role of ZnPc layer in the ITO/PTCBI/CoPc/ZnPc in photocurrent measurements, incidence was controlled using a blue filter (B390), where the light of wavelength $\lambda > 510$ nm can be cut off. That is, the B390 filter was used to prevent absorption of CoPc and ZnPc (cf. Fig. 2(b)).
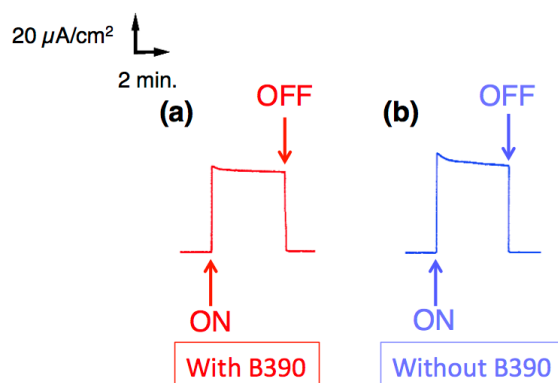

Figure 3. Photocurrents measured at ITO/PTCBI/CoPc/ZnPc with (a) and without (b) a band-pass filter. A single-compartment cell was employed in this study, similar to the studies in Figures 1 and 2. Film thickness, ~260 nm for PTCBI, ~50 nm for CoPc and ~30 nm for ZnPc; electrolyte solution, 5 mM Cys solution (pH 10); light intensity, 38 mW·cm^{-2}; irradiation direction: from the back side of the ITO-coated face; type of band-pass filter, B390; applied potential, +0.4 V vs. Ag/AgCl (sat.).

Fig. 3 shows the photocurrents measured under the potentiostatic and constant light-intensity conditions with (a) and without (b) the filter. In both cases, photocurrent of the same magnitude was monitored. This observation indicates that no absorption of phthalocyanines contributes to the photocurrent generation, thus suggesting that ZnPc can act as a hole-conducting layer (p-type conductor).

Table 1. Electrolye solutions employed for voltammetric measurements

|	Types of amino acids	pH	Note[a]
Entry 1	Cys	6.0	Almost all of the –COOH groups in Cys are dissociated.
Entry 2	Ser	6.0	Almost all of the –COOH groups in Ser are dissociated.
Entry 3	Cys	8.7	Almost all of the –NH$_2$ groups in Cys remain protonated.
Entry 4	Ser	8.5	The concentration of the –NH$_2$ group is the same condition as Fig. 1 (i.e. in the presence of Cys at pH 10). In both cases, the –NH$_2$ concentration is constant (i.e. 1 mM).

a) Total concentration of an amino acid was 5 mM in each experiment.
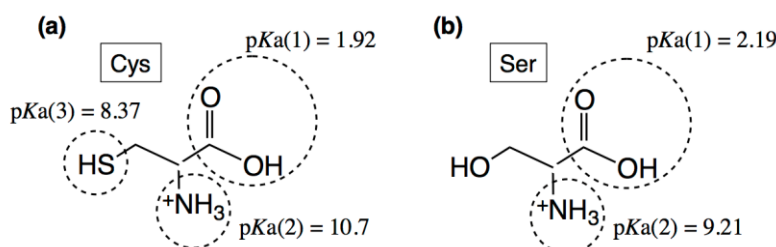
Figure 4. Acid dissociation constants of Cys (a) and Ser (b). The pKa(1), pKa(2), and pKa(3) values represent those of carboxy group, protonated amino group, and thiol group, respectively.
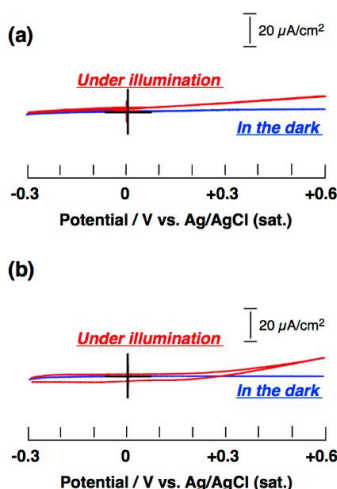
Figure 5. Cyclic voltammograms measured at ITO/PTCBI/CoPc in the presence of Cys (a) or Ser (b). A single-compartment cell was employed in this experiment, similar to the experiment in Figure 1. Film thickness, ~230 nm for PTCBI and ~55 nm for CoPc; amino acid concentrations, 5 mM (pH 6); light intensity, 100 mW·cm^{-2}; irradiation direction: from the back side of the ITO-coated face; scan rate, 20 mV·s^{-1}.
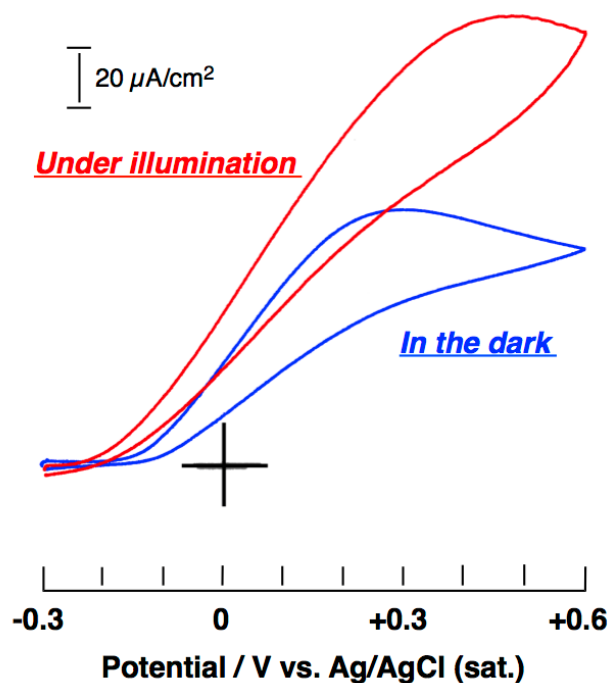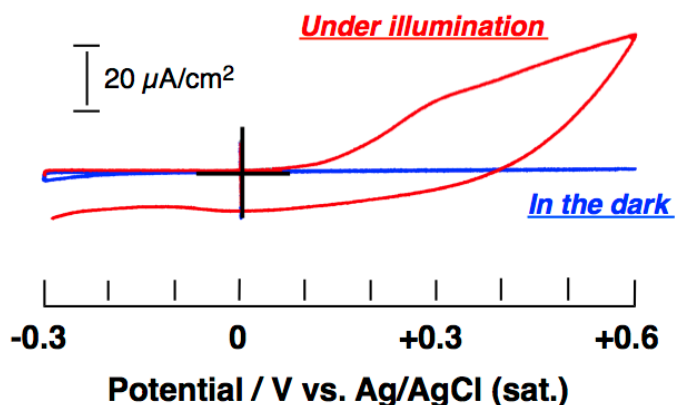
Figure 6. Cyclic voltammograms measured at ITO/PTCBI/CoPc in the presence of Cys. A single-compartment cell was employed in this experiment, similar to the experiments in Fig. 5. Film thickness, ~240 nm for PTCBI and ~60 nm for CoPc; Cys concentration, 5 mM (pH 8.7); light intensity, 100 mW·cm^{-2}; irradiation direction: from the back side of the ITO-coated face; scan rate, 20 mV·s^{-1}.

Next, we have identified the functional groups of Cys subjected to the dual catalysis by ITO/PTCBI/CoPc. Therefore, employing Ser as a reference compound, controlled experiments were performed in terms of voltammetry. Ser and Cys exhibit a similar structure, but a thiol group (–SH) of Cys is replaced by hydroxy group (–OH) in Ser. A list of the experimental conditions is shown in Table 1.

Additionally, dissociation constants of the functional groups of the amino acids are presented in Fig. 4 [29]. Entries 1 and 2 correspond to the conditions where only the terminal carboxy group is dissociated. As shown in Fig. 5, irrespective of types of amino acids employed, no response was observed under illumination and in the dark, indicating that the carboxylate anion (–COO$^-$) in both Cys and Ser is inactive in the dual catalysis. In Entry 3 where almost all of the protonated amino groups (i.e. –NH$_3{}^+$) in Cys remain undissociated and the thiolate anion (i.e. –S$^-$) is in relatively low concentration (Fig. 6), both photoanodic and anodic responses were qualitatively observed to occur at ITO/PTCBI/CoPc, similar to Fig. 1(a). Entry 4 corresponds to the conditions where the concentration of the amino group (–NH$_2$) in Ser is the same as in the experiments shown in Fig. 1 (cf. in that case, the –NH$_2$ concentration was calculated to be 1 mM). However, the photoanodic response depicted in Fig. 7 was inferior to that of Fig. 1, and moreover, no response was detected in the dark. These results suggest that dual catalysis by the organo-bilayer cannot occur for the –NH$_2$ group in each amino acid. Based on the aforementioned results, it appeared that the species subjected to dual catalysis, as shown in Fig. 1(a), is the –S$^-$ species of Cys.

Figure 7. Cyclic voltammograms measured at ITO/PTCBI/CoPc in the presence of Ser. A single-compartment cell was employed in this experiment, similar to the experiments in Fig. 5. Film thickness, ~230 nm for PTCBI and ~60 nm for CoPc; Ser concentration, 5 mM (pH 8.5); light intensity, 100 mW·cm^{-2}; irradiation direction: from the back side of the ITO-coated face; scan rate, 20 mV·s^{-1}.

Potentiostatic electrolysis was performed under the similar conditions as for the experiments depicted in Fig. 1(a), where molecular hydrogen (H$_2$) was reductively produced along with the oxidation of the thiolate anion (Scheme 2).
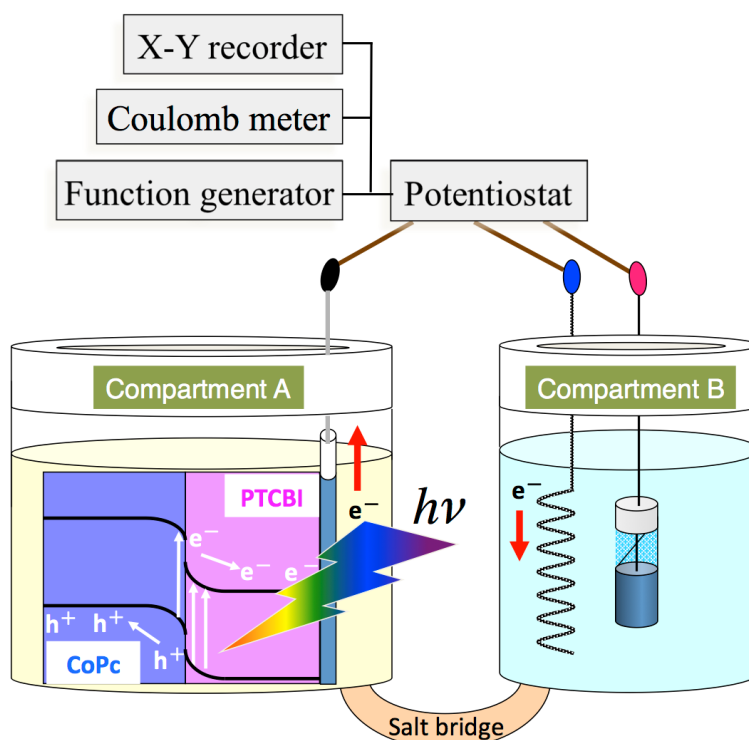
Scheme 2. The electrolysis system composed of ITO/PTCBI/CoPc (or ITO/PTCBI/CoPc/ZnPc), Pt counter, and Ag/AgCl (sat.).

The electrolysis data are presented in Table 2.

Table 2. The electrolysis data for the system depicted in Scheme 2

	System	H_2 amount / μL	Note
Entry 1[a]	ITO/PTCBI/CoPc	74.0	With irradiation
Entry 2[a]	ITO/PTCBI/CoPc	32.4	Without irradiation
Entry 3[a,b]	ITO/PTCBI/CoPc/ZnPc	47.8	With irradiation
Entry 4[a,b]	ITO/PTCBI/CoPc/ZnPc	1.10	Without irradiation

a) Film thickness, PTCBI = ~260 nm and CoPc = ~50 nm; total concentration of Cys in the compartment A, 5 mM (pH 10); electrolyte solution in the compartment B, H_2PO_4 solution (pH 0); applied potential, +0.3 V vs. Ag/AgCl (sat.); light intensity, 100 mW·cm^{-2}; electrolysis time, 1 hours.
b) In addition to the conditions employed in *a)*, ZnPc (~35 nm) was further loaded on the CoPc surface in the PTCBI/CoPc bilayer.

As expected from the voltammogram measurements depicted in Fig. 1(a), the redox reaction occurred in the dark, and increasing amounts of H_2 were also observed under illumination (Entries 1 and 2). Furthermore, when employing the organo-trilayer of ITO/PTCBI/CoPc/ZnPc as the anode, the net amount of H_2 evolved under irradiation was confirmed (i.e. Entry 1–Entry 2 ≈ Entry 3–Entry 4). These results demonstrate that the ITO/PTCBI/CoPc electrode is active for the oxidation of the thiolate anion in Cys, regardless of irradiation.

Catalytic reaction was also conducted under the same conditions as those for electrolysis, according to Scheme 1, where no electrochemical potential was applied to the system. Similar to the electrolysis data of Table 2, the evolution of H_2 catalytically occurred both under illumination and in the dark (Table 3).

Table 3. The catalysis data for the system depicted in Scheme 1

	System	H_2 amount / μL	Note
Entry 1[a]	ITO/PTCBI/CoPc	12.1	With irradiation
Entry 2[a]	ITO/PTCBI/CoPc	4.80	Without irradiation
Entry 3[a,b]	ITO/PTCBI/CoPc/ZnPc	9.71	With irradiation
Entry 4[a,b]	ITO/PTCBI/CoPc/ZnPc	0	Without irradiation

a) Film thickness, PTCBI = ~240 nm and CoPc = ~45 nm; total concentration of Cys in the compartment A, 5 mM (pH 10); electrolyte solution in the compartment B, H_2PO_4 solution (pH 0); light intensity, 100 mW·cm^{-2}; electrolysis time, 3 hours.
b) In addition to the conditions employed in *a)*, ZnPc (~30 nm) was further loaded on the CoPc surface in the PTCBI/CoPc bilayer.

On the other hand, in the control experiments where the single-layered PTCBI or CoPc was used, no evolution of H_2 was confirmed, irrespective of irradiation. The details of the dual-catalysis mechanism have been recently described in our report (also see INTRODUCTION) [20]. Thus, the data of Table 3 proved that the dual catalysis by ITO/PTCBI/CoPc occurs resulting in the oxidation of the thiolate anion of Cys along with the reduction of H^+.

4. CONCLUSION

We have demonstrated that the PTCBI/CoPc bilayer can catalytically induce the oxidation of a thiolate anion of Cys along with the reduction of H^+ to H_2, both in the dark and under illumination. It evidenced that the organo-bilayer shows similar dual-catalysis activity for the cysteine oxidation in the comparison with our recent instance of 2-mercaptoethanol oxidation [20]. In addition to a few photocatalysts [30-33], a large number of papers are reported with regards to catalysts capable of thiols oxidation in the dark [34-41], but there is no report of the dual catalysis by other groups. Such dual-functional catalysis by the organo-bilayer can occur effectively for a down-hill reaction, where the distinct oxidation states of a p-type organic semiconductor are advantageously available for oxidation (at the bottom end of the conduction band for catalysis in the dark and at the top end of the valence band for catalysis under illumination). The dual catalysis is a novel approach that has not yet been employed to conventional photocatalysts. What types of organo-bilayers can catalyze what kinds of substances and pollutants must be investigated in the future.

References

1. L. Jiang, X. Yuan, G. Zeng, Z. Wu, J. Liang, X. Chen, L. Leng and H. Wang, H. Wang, *Appl. Catal.*, *B*, 221 (2018) 715.
2. U. Alam, S. Kumar, D. Bahnemann, J. Koch, C. Tegenkamp and M. Muneer, *Phys. Chem. Chem. Phys.*, 20 (2018) 4538.
3. F. Ma, Q. Yang, Z. Wang, Y. Liu, J. Xin, J. Zhang, Y. Hao and L. Li, *RSC Adv.*, 5 (2018) 15853.
4. Y. Huang, Y. Lu, Y. Lin, Y. Mao, G. Ouyang, H. Liu, S. Zhang and Y. Tong, *J. Mater. Chem. A*, 6 (2018) 24740.
5. L.K. Dhandole, S.-G. Kim., Y.-S. Seo., M.A. Nahadik, H.S. Chung, S.Y. Lee, S.H. Choi, M. Cho, J. Ryu and J.S. Jang, *ACS Sustainable Chem. Eng.*, 6 (2018) 4302.
6. Y. Goto, T. Hisatomi, Q. Wang, T. Higashi, K. Ishikiriyama, T. Maeda, Y. Sakata, S. Okunaka, H. Tokudome, M. Katayama, S. Akiyama, H. Nishiyama, Y. Inoue, T. Takewaki, T. Setoyama, T. Minegishi, T. Takata, T. Yamada and K. Domen, *Joule*, 2 (2018) 509.
7. M. Zhu, Z. Sun, M. Fujitsuka and T. Majima, *Angew. Chem.*, *Int. Ed.*, 57 (2018) 2160.
8. Y. Fu, C. Zhu, C. Liu, M. Zhang, H. Wang, W. Shi, H. Huang, Y. Liu and Z. Kang, *Appl. Catal.*, *B*, 226 (2018) 295.
9. A. Bloesser, P. Voepel, M.O. Loeh, A. Beyer, K. Volz and R. Marschall, *J. Mater. Chem. A*, 6 (2018) 1971.
10. X. Sun, Y. Mi, F. Jiao and X. Xu, *ACS Catal.*, 8 (2018) 3209.
11. Y. Ye, Y. Feng, H. Bruning, D. Yntema and H.H.M. Rijnaarts, *Appl. Catal.*, *B*, 220 (2018) 171.
12. H. Zhu, N. Goswami, Q. Yao, T. Chen, Y. Liu, Q. Xu, D. Chen, J. Lu and J. Xie, *J. Mater. Chem. A*, 6 (2018) 1102.
13. J. Zhang, Y. Cai, X. Hou, H. Zhou, H. Qiao and Q. Wei, *J. Phys. Chem. C*, 122 (2018) 8946.
14. D. Mendori, T. Hiroya, M. Ueda, M. Sanyoushi, K. Nagai and T. Abe, *Appl. Catal., B*, 205 (2017)

514.
15. K. Fujine, Y. Sato, K. Nagai and T. Abe, *J. Electroanal. Chem.*, 823 (2018) 322-327.
16. T. Abe, J. Chiba, M. Ishidoya and K. Nagai, *RSC Adv.*, 2 (2012) 7992.
17. T. Abe, N. Taira, Y. Tanno, Y. Kikuchi and K. Nagai, *Chem. Commun.*, 50 (2014) 1950.
18. T. Abe, Y. Tanno, N. Taira and K. Nagai, *RSC Adv.*, 5 (2015) 46325.
19. T. Abe, K. Fukui, Y. Kawai, K. Nagai and H. Kato, *Chem. Commun.*, 52 (2016) 7735.
20. T. Abe, M. Okumura, Y. Kikuchi, T. Itoh and K. Nagai, *J. Mater. Chem. A*, 5 (2017) 7445.
21. T. Maki and H. Hashimoto, *Bull. Chem. Soc. Jpn.*, 25 (1952) 411.
22. T. Morikawa, C. Adachi, T. Tsutsui and S. Saito, *Nippon Kagaku Kaishi*, (1990) 962.
23. N. Ohta and M. Gomi, *Jpn. J. Appl. Phys.*, 39 (2000) 4195.
24. H. Yoshida, Y. Tokura and T. Koda, *Chem. Phys.*, 109 (1986) 375.
25. T. Abe, K. Nagai, S. Kabutomori, M. Kaneko, A. Tajiri and T. Norimatsu, *Angew. Chem.*, *Int. Ed.*, 45 (2006) 2778.
26. T. Abe, S. Miyakushi, K. Nagai and T. Norimatsu, *Phys. Chem. Chem. Phys.*, 10 (2008) 1562.
27. T. Abe, S. Tobinai, N. Taira, J. Chiba, T. Itoh and K. Nagai, *J. Phys. Chem. C*, 115 (2011) 7701.
28. K. Nagai, Y. Fujimoto, H. Shiroishi, M. Kaneko, T. Norimatsu and T. Yamanaka, *Chem. Lett.*, (2001) 354.
29. https://www.nacalai.co.jp/information/trivia2/11.html
30. S. Naya, M. Teranishi, T. Isobe and H. Tada, *Chem. Commun.*, 46 (2010) 815.
31. C. Bottecchia, N. Erdmann, P.M.A. Tijssen, L.G. Milroy, L. Brunsveld, V. Hessel and T. Noël, *ChemSusChem*, 9 (2016) 1781.
32. L.V. Lutkus, H.E. Irving, K.S. Davies, J.E. Hill, J.E. Lohman, M.W. Eskew, M.R. Detty and T.M. McCormick, *Organometallics*, 36 (2017) 2588.
33. W.-B. Wu, Y.-C. Wong, Z.-K. Tan and J. Wu, *Catal. Sci. Technol.*, 8 (2018) 4257.
34. H. Shirai, H. Tsuiki, E. Masuda, T. Koyama, K. Hanabusa and N. Kobayashi, *J. Phys. Chem.*, 95 (1991) 417.
35. A. Corma, V. Fornes, F. Rey, A. Cervilla, E. Llopis and A. Ribera, *J. Catal.*, 152 (1995) 237.
36. M.M. Abu-Omar and S.I. Khan, *Inorg. Chem.*, 37 (1998) 4979.
37. M. Hassanein, H. El-Hamshary, N. Salahuddin and A. Abu-El-Fotoh, *J. Mol. Catal. A: Chem.*, 234 (2005) 45.
38. E. Golub, R. Freeman and I. Willner, *Anal. Chem.*, 85 (2013) 12126.
39. M.G. Gantman, J.G. Tarkhanova and Y.G. Kolyagin, *J. Sulfur Chem.*, 37 (2016) 501.
40. R. Tamura, T. Kawata, Y. Hattori, N. Kobayashi and M. Kimura, *Macromolecules*, 50 (2017) 7978.
41. X. Chen, C. McGlynn and A.R. McDonald, *Chem. Mater.*, 30 (2018) 6978.